Hindawi
Complexity
Volume 2019, Article ID 7289689, 12 pages
https://doi.org/10.1155/2019/7289689

Research Article

σ-Stabilization of a Flexible Joint Robotic Arm via Delayed Controllers

G. Ochoa-Ortega,[1] **R. Villafuerte-Segura**,[2] **M. Ramírez-Neria**,[1,3] **and L. Vite-Hernández**[2]

[1]*División de Mecatrónica, Universidad Politécnica del Valle de México, Tultitlán 54910, Mexico*
[2]*Centro de Investigación en Tecnologías de Información y Sistemas, Universidad Autónoma del Estado de Hidalgo, Pachuca 42184, Hidalgo, Mexico*
[3]*Departamento de Mecatrónica, Universidad Tecnológica de México-UNITEC MÉXICO-Campus Atizapán, Atizapán de Zaragoza 52999, Mexico*

Correspondence should be addressed to R. Villafuerte-Segura; villafuerte@uaeh.edu.mx

Received 7 September 2019; Revised 6 November 2019; Accepted 28 November 2019; Published 23 December 2019

Academic Editor: Thach Ngoc Dinh

In the present contribution, the problem of establishing tuning rules to proportional retarded controller for LTI systems is addressed. Based on the $\mathcal{D}$-decomposition methodology and σ-stability analysis, analytic conditions are determined on the parameters of a delayed controller that guarantee us that the system response reaches the maximal decay rate. The conditions presented in this paper are tested experimentally in tracking tasks of a flexible joint robotic arm.

1. Introduction

Time delays naturally arise in many mathematical models from engineering, biology, and physics, among other science areas. A common belief is that the appearance of these phenomena can lead to detrimental effects, bad performance of the system, instability, or even damage to the system [1]. Nevertheless, many contributions have shown that the deliberate introduction of a time delay in a feedback control law can provide a stabilizing effect [2–7] and in some cases give or improve the robustness property of the system [8]. The stability analysis of linear time delay systems is studied in the framework of two main approaches: time domain and frequency domain. The former is based on the well-known Lyapunov's criteria and its extensions (Razumikhin and Krasovskii) or by using linear matrix inequalities (LMIs) via convex optimization [9, 10]. However, only sufficient stability conditions are provided, which are generally very conservative or, in some cases, nonexistent, mainly because the feasibility of LMIs (whose parameters are adjusted by a frequency method) is usually nonexistent. The second approach is based on the analysis of the characteristic function of the system, where, unlike the temporal approach, it is possible to provide necessary and sufficient conditions that do not have a conservative nature.

Even when in the recent decades there is a great development in the control theory, where many sophisticated control schemes have been developed, PID controllers remain as one of the most used control strategies in the industrial environment. According to [11, 12], approximately 90–95% of the industrial control loops still use PID-type controllers, many of which do not include the derivative term, mainly because this term induces a noise amplifying effect that can affect the system performance [12–14] or because the derivative of the state is not available for measurement. Some common strategies to avoid the use of the derivative term and, consequently, the noise amplification problem, are the use of filters, and observers or the implementation of estimation schemes.

On the other hand, a common approach consists in replacing the derivative term in PID-type controllers by an approximation of the form

$$\frac{\mathrm{d}x(t)}{\mathrm{d}t} \approx \frac{x(t) - x(t-\tau)}{\tau}, \tag{1}$$

and for an appropriate selection of the delay τ, the closed-loop stability is guaranteed [3, 14–16]. In this framework, in [17], a method for the migration of a double imaginary characteristic root to the left half-plane or the right half-plane under the variation of two parameters of a quasi-polynomial is presented. The idea of deliberately introducing time delays in closed-loop systems and considering it as a control parameter is not a novel approach, but it has been intensively studied in recent years, see [18–20] and the references therein. The analysis of such class of controllers focuses mainly on the following topics: characterization of the stability crossing curves [21], tuning of delayed controllers to stabilize second-order systems [18, 20, 22] (and its noise attenuation analysis [23]), the design of proportional integral controllers for second-order linear systems [19, 24], and design of maximum decay rate using elimination theory [25]. Particularly in [26], a Proportional Integral Retarded (PIR) controller to solve the regulation problem of a general class of stable second-order LTI systems is presented. This result ultimately guarantees a desired exponential decay rate σ. On the other hand, design of nonfragile controllers with a desired exponential decay rate is proposed in [20]. Here, the authors present conditions on the parameters (k_p, k_δ) such that the $p-\delta$ controller of the form $k_p + k_\delta e^{-\tau s}$ ensure the stability of the closed-loop system.

Inspired by the previous contributions, in the present manuscript, following the $\mathscr{D}$-decomposition methodology (see [27–30]), it allows us to delimit and decompose the space of control parameters, determining the stability boundaries by means of a set of parametric equations that depends explicitly on the control parameters, which play a key step to allow us to determine simple analytical expressions for tuning the control parameters of a Proportional Retarded (PR) control law to σ-stabilize a general class of SISO LTI systems. Under these conditions, three dominant real roots are placed in $-\sigma$, which guarantees to reach the maximal exponential decay rate in the system response.

The σ-stabilization of a system can be described as the design and tuning of a controller such that the corresponding characteristic equation of the closed-loop system has dominant roots with real part less than or equal to $-\sigma$, $\sigma \in \mathbb{R}^+$. The σ-stabilization approach can be considered a robust scheme, since when taking parameters within a σ-stable region and by presenting variations on the parameters (that do not leave the σ-stable zone) the system stability is assured.

Delay-based controllers have as their main advantages the simplicity with which control laws are designed and, as a consequence, their practical implementation facility. Common applications of such controllers focus mainly on second-order systems, e.g., regulation problems of DC servomotors [18, 31], haptic virtual systems [20], underactuated mechanical system [32], and numerous academic examples. In the present proposal, a more challenging implementation is addressed: a flexible joint robotic arm (fourth order system), where trajectory tracking tasks are addressed. The main challenges for the design of PR control law are the complexity of its dynamic equations (mainly by the presence of highly nonlinear elements) and the appearance of oscillations at the tip of the link [33, 34]. Thus, a first step in the design of the Proportional Retarded control law is to linearize via an exact linearization approach the dynamic equations of the flexible joint robotic arm [35, 36].

The remainder of this manuscript is organized as follows. In Section 2, the analyzed closed-loop system and the problem formulation are presented and the σ-stability boundaries are determined. In Section 3, analytic conditions to determine the maximal decay rate σ^* are provided. Section 4 is devoted to both the dynamic model of the flexible joint robotic arm under the study and the design of the proportional plus delay controller. Also, a complementary tuning approach is presented. In Section 5, the experimental platform is described and the experimental results are presented. For comparison purposes, a classical feedback state controller law is also designed and implemented. The contributions end with some concluding remarks.

Nomenclature. In the present contribution, $\mathbb{R}$ denotes the real numbers, while $\mathbb{C}$ the complex numbers, and Z^+ stands for the positive integers. Given a vector $x(t) \in \mathbb{R}^n$, then $x(t)^\top$ denotes its transpose. Let $s \in \mathbb{C} \mid s = a + ib$, then $\mathrm{Re}(s) = a$ and $\mathrm{Im}(s) = b$ denote its real and imaginary parts of s, respectively, and i is the imaginary unit. For a function $x(t)$, $\dot{x}(t)$ denotes its time derivative and $\mathrm{d}^k x(t)/\mathrm{d}t^j = x^{(j)}(t)$ and $j \in \mathbb{Z}^+$ defines the jth time derivative.

2. Problem Formulation

Let us consider a LTI-SISO system of the form

$$\dot{x}(t) = Ax(t) + Bu(t), \tag{2}$$

where $A \in \mathbb{R}^{n\times n}$, $B \in \mathbb{R}^n$, $x(t) = [x_1(t), x_2(t), \ldots, x_n(t)]^\top \in \mathbb{R}^n$, and $u(t) \in \mathbb{R}$ is the control input. Let us propose a state feedback a control law of the form

$$u(t) = \widetilde{k}_1 x_1(t) + \widetilde{k}_2 x_2(t) + \cdots + \widetilde{k}_n x_n(t), \tag{3}$$

where $\widetilde{k}_j \in \mathbb{R}$, $j = 1, 2, \ldots, n$, denote the controller gains. This approach demands the knowledge of the complete state vector. Now, let us suppose that at least one of the velocity measurements is not available, and then the implementation of a state observer to estimate the unavailable states would be considered. Instead of this alternative, let us propose a delayed controller as follows:

$$u(t) = k_p x_1(t) - k_r x_1(t-\tau) + \alpha_1 x_3(t) + \cdots + \alpha_{n-2} x_n(t), \tag{4}$$

where k_p, k_r, $\alpha_1 \ldots, \alpha_{n-2} \in \mathbb{R}$ are the controller gains, and $\tau > 0$ is the delay. Here, we assume that the state variable $x_2(t)$ is unable to measure. Then, the closed-loop system is now of form

$$\dot{x}(t) = A_0 x(t) + A_1 x(t-\tau), \tag{5}$$

where $A_0, A_1 \in \mathbb{R}^{n\times n}$. Then, the characteristic function of system (5) is

$$Q\left(s, k_p, k_r, \alpha_1, \ldots, \alpha_{n-2}\right) = p\left(s, k_p, \alpha_1, \ldots, \alpha_{n-2}\right) + k_r q(s) e^{-s\tau}, \tag{6}$$

where $p(\cdot)$ and $q(\cdot)$ are polynomials and $s \in \mathbb{C}$.

In the subsequent sections, analytic conditions will be developed on the control parameters k_r and τ that guarantee a maximal exponential decay rate (denoted by σ^*) on the system response.

3. Decomposition of the Gain Controller Parametric Space

As discussed in the introductory section, a key step to determine the analytic conditions on the parameters to achieve the maximal decay rate is the decomposition of the space of parameters by means of the $\mathscr{D}$-decomposition methodology. To this end, we first study the σ-stability or stability degree $\sigma > 0$ of (6). Then, let us consider $\sigma > 0$ and by proposing the change of variable, $s \longrightarrow (s - \sigma)$, quasi-polynomial (6) takes the form

$$\begin{aligned} Q_\sigma\left(s, k_p, k_r, \alpha_1, \ldots, \alpha_{n-2}\right) &\coloneqq Q\left(s - \sigma, k_p, k_r, \alpha_1, \ldots, \alpha_{n-2}\right) \\ &= p\left(s, k_p, \alpha_1, \ldots, \alpha_{n-2}, \sigma\right) \\ &\quad + k_r e^{\sigma\tau} q(s, \sigma) e^{-s\tau}. \end{aligned} \tag{7}$$

Following the $\mathscr{D}$-decomposition methodology, we first compute $Q_\sigma(\cdot)|_{s=0} = 0$:

$$p\left(0, k_p, \alpha_1, \ldots, \alpha_{n-2}, \sigma\right) + k_r e^{\sigma\tau} q(0, \sigma) = 0, \tag{8}$$

since $p(0, k_p, \alpha_1, \ldots, \alpha_{n-2}, \sigma) \neq 0$ and $q(0, \sigma) \neq 0$, then

$$k_r = -\frac{p\left(0, k_p, \alpha_1, \ldots, \alpha_{n-2}, \sigma\right)}{e^{\sigma\tau} q(0, \sigma)}. \tag{9}$$

Now, evaluating $Q_\sigma(\cdot)$ for $s = i\omega$, $\omega > 0$, results

$$p\left(i\omega, k_p, \alpha_1, \ldots, \alpha_{n-2}, \sigma\right) + k_r e^{\sigma\tau} q(i\omega, \sigma) e^{-i\omega\tau} = 0, \tag{10}$$

or in an equivalent form:

$$-\frac{1}{k_r e^{\sigma\tau}} \left(\frac{p\left(i\omega, k_p, \alpha_1, \ldots, \alpha_{n-2}, \sigma\right)}{q(i\omega, \sigma)} \right) = e^{-i\omega\tau}. \tag{11}$$

Then, from Euler's identity, it follows that

$$\begin{aligned} \cos(\omega\tau) &= -\frac{1}{k_r e^{\sigma\tau}} \operatorname{Re}\left\{ \frac{p\left(i\omega, k_p, \alpha_1, \ldots, \alpha_{n-2}, \sigma\right)}{q(i\omega, \sigma)} \right\}, \\ \sin(\omega\tau) &= \frac{1}{k_r e^{\sigma\tau}} \operatorname{Im}\left\{ \frac{p\left(i\omega, k_p, \alpha_1, \ldots, \alpha_{n-2}, \sigma\right)}{q(i\omega, \sigma)} \right\}, \end{aligned} \tag{12}$$

and from the former equations, an explicit expression for τ can be written as follows:

$$\tau = \frac{1}{\omega} \cot^{-1}\left(-\frac{\operatorname{Re}\left\{ \left(p\left(i\omega, k_p, \alpha_1, \ldots, \alpha_{n-2}, \sigma\right) \right) / \left(q(i\omega, \sigma) \right) \right\}}{\operatorname{Im}\left\{ \left(p\left(i\omega, k_p, \alpha_1, \ldots, \alpha_{n-2}, \sigma\right) \right) / q(i\omega, \sigma) \right\}} \right) + \frac{j\pi}{\omega}, \tag{13}$$

for $j = 0, \pm 1, \pm 2, \ldots$. Finally from equation (12) yields

$$k_r = \frac{1}{e^{\sigma\tau} \sin(\omega\tau)} \operatorname{Im}\left\{ \frac{p\left(i\omega, k_p, \alpha_1, \ldots, \alpha_{n-2}, \sigma\right)}{q(i\omega, \sigma)} \right\}. \tag{14}$$

The above analysis is summarized in the following result.

Proposition 1. *Consider a quasi-polynomial of form (6), and then the σ-stability regions are bounded by the following equations.*

When $s = 0$,

$$k_r = -\frac{p\left(0, k_p, \alpha_1, \ldots, \alpha_{n-2}, \sigma\right)}{e^{\sigma\tau} q(0, \sigma)}, \quad \tau \in \mathbb{R}^+, \tag{15}$$

and for $s = i\omega$

$$\tau = \frac{1}{\omega} \cot^{-1}\left(-\frac{\operatorname{Re}\left\{ \left(p\left(i\omega, k_p, \alpha_1, \ldots, \alpha_{n-2}, \sigma\right) \right) / \left(q(i\omega, \sigma) \right) \right\}}{\operatorname{Im}\left\{ \left(p\left(i\omega, k_p, \alpha_1, \ldots, \alpha_{n-2}, \sigma\right) \right) / \left(q(i\omega, \sigma) \right) \right\}} \right) + \frac{j\pi}{\omega}, \tag{16}$$

$$k_r = \frac{1}{e^{\sigma\tau} \sin(\omega\tau)} \operatorname{Im}\left\{ \frac{p\left(i\omega, k_p, \alpha_1, \ldots, \alpha_{n-2}, \sigma\right)}{q(i\omega, \sigma)} \right\}, \tag{17}$$

where, $j = 0, \pm 1, \pm 2, \ldots$. Expressions (15)–(17) of Proposition 1 define the σ-stability boundaries in the parametric space (τ, k_r). To exemplify these stability boundaries, in Figure 1, a generic parametric map is presented. The outer region denotes the stability boundary of the system, that is, it corresponds to the pair (τ, k_r) for which the eigenvalues of the system lies on the imaginary axis, while each one of the inner contour curves define a region where the system is exponentially stable with a specific decay rate $\sigma > 0$. The red point corresponds to the maximal reachable stability degree, denoted by σ^*, and it occurs when all the σ-stable regions collapse in a single point (τ^*, k_r^*) of the parametric space and it is characterized because the characteristic function present a root of multiplicity at least three at $s = \sigma^*$ (see [22, 26]).

In the next section, analytic expressions to determine the maximal decay rate σ^* and the associated parameters (τ^*, k_r^*) are presented.

4. Tuning of the PR Control Law

In this section, analytic expressions for determining the controller parameters τ^*, k_r^*, and σ^* to reach the maximal decay rate are provided.

Proposition 2. *Let us consider a quasi-polynomial of form (6), then it has a dominant root of multiplicity at least three at the point $s = -\sigma^*$, if σ^* is the smallest positive real root of the polynomial:*

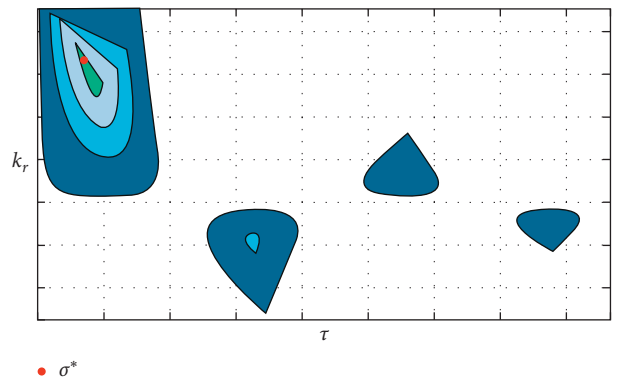

Figure 1: (τ, k_r) parametric space.

$$f(\sigma) = \frac{1}{p\left(0, k_p, \alpha_1, \ldots, \alpha_{n-2}, \sigma\right)}\left[\frac{\partial p\left(s, k_p, \alpha_1, \ldots, \alpha_{n-2}, \sigma\right)}{\partial s} - \frac{p\left(0, k_p, \alpha_1, \ldots, \alpha_{n-2}, \sigma\right)}{q(0,\sigma)}\frac{\partial q(s,\sigma)}{\partial s}\right]^2\Bigg|_{s=0}$$
$$+\frac{2}{q(0,\sigma)}\frac{\partial q(s,\sigma)}{\partial s}\left[\frac{\partial p\left(s, k_p, \alpha_1, \ldots, \alpha_{n-2}, \sigma\right)}{\partial s} - \frac{p\left(0, k_p, \alpha_1, \ldots, \alpha_{n-2}, \sigma\right)}{q(0,\sigma)}\frac{\partial q(s,\sigma)}{\partial s}\right]\Bigg|_{s=0} \tag{18}$$
$$+\left[\frac{p\left(0, k_p, \alpha_1, \ldots, \alpha_{n-2}, \sigma\right)}{q(0,\sigma)}\frac{\partial^2 q(s,\sigma)}{\partial s^2}\right]\Bigg|_{s=0} - \left[\frac{\partial^2 p\left(s, k_p, \alpha_1, \ldots, \alpha_{n-2}, \sigma\right)}{\partial s^2}\right]\Bigg|_{s=0} = 0,$$

and the delay $\tau = \tau(\sigma^*)$ and the controller gain $k_r = k_r(\sigma^*, \tau)$ satisfy the following relations:

$$\tau = -\frac{1}{p\left(0, k_p, \alpha_1, \ldots, \alpha_{n-2}, \sigma\right)}\left[\frac{\partial p\left(s, k_p, \alpha_1, \ldots, \alpha_{n-2}, \sigma\right)}{\partial s} - \frac{p\left(0, k_p, \alpha_1, \ldots, \alpha_{n-2}, \sigma\right)}{q(0,\sigma)}\frac{\partial q(s,\sigma)}{\partial s}\right]\Bigg|_{s=0},$$
$$k_r = -\frac{\left(\partial p\left(s, k_p, \alpha_1, \ldots, \alpha_{n-2}, \sigma\right)\right)/(\partial s)\big|_{s=0}}{e^{\sigma\tau}\left[\left(\partial q(s,\sigma)\right)/(\partial s)\,|_{s=0} - \tau q(0,\sigma)\right]}. \tag{19}$$

Proof 1. If quasi-polynomial (7) has three dominant roots in $s = 0$, it implies that quasi-polynomial (6) has three dominant roots at $s = -\sigma$. Thus, conditions $Q_\sigma(\cdot)|_{s=0} = 0$, $(\partial/\partial s)Q_\sigma(\cdot)|_{s=0} = 0$, and $(\partial^2/\partial s^2)Q_\sigma(\cdot)|_{s=0} = 0$ must hold, i.e.,

$$0 = Q_\sigma(\cdot)_{|s=0} = p\left(0, k_p, \alpha_1, \ldots, \alpha_{n-2}, \sigma\right) + k_r e^{\sigma\tau} q(0,\sigma), \tag{20}$$

$$0 = \frac{\partial}{\partial s}Q_\sigma(\cdot)\Big|_{s=0} = \left[\frac{\partial p\left(s, k_p, \alpha_1, \ldots, \alpha_{n-2}, \sigma\right)}{\partial s} + k_r e^{\sigma\tau}\left[\frac{\partial q(s,\sigma)}{\partial s} - \tau q(s,\sigma)\right]e^{-s\tau}\right]\Bigg|_{s=0}, \tag{21}$$

$$0 = \frac{\partial^2}{\partial s^2}Q_\sigma(\cdot)\Big|_{s=0} = \left[\frac{\partial^2 p\left(s, k_p, \alpha_1, \ldots, \alpha_{n-2}, \sigma\right)}{\partial s^2} + k_r e^{\sigma\tau}\left[\frac{\partial^2 q(s,\sigma)}{\partial s^2} - 2\tau\frac{\partial q(s,\sigma)}{\partial s} + \tau^2 q(s,\sigma)\right]e^{-s\tau}\right]\Bigg|_{s=0}. \tag{22}$$

Condition (19) follows directly from (21). Now, through direct computations, it can be verified that equations (20) and (21) lead us to

$$\tau = -\frac{1}{p\left(0, k_p, \alpha_1, \ldots, \alpha_{n-2}, \sigma\right)}\left[\frac{\partial p\left(s, k_p, \alpha_1, \ldots, \alpha_{n-2}, \sigma\right)}{\partial s} - \frac{p\left(0, k_p, \alpha_1, \ldots, \alpha_{n-2}, \sigma\right)}{q(0,\sigma)}\frac{\partial q(s,\sigma)}{\partial s}\right]\Bigg|_{s=0}. \tag{23}$$

On the other hand, equations (20) and (22), imply that

$$0 = \left[\tau^2 p\left(0, k_p, \alpha_1, \ldots, \alpha_{n-2}, \sigma\right) - 2\tau\frac{p\left(0, k_p, \alpha_1, \ldots, \alpha_{n-2}, \sigma\right)}{q(0,\sigma)}\frac{\partial q(s,\sigma)}{\partial s} - \frac{\partial^2 p\left(s, k_p, \alpha_1, \ldots, \alpha_{n-2}, \sigma\right)}{\partial s^2} + \frac{p\left(0, k_p, \alpha_1, \ldots, \alpha_{n-2}, \sigma\right)}{q(0,\sigma)}\frac{\partial^2 q(s,\sigma)}{\partial s^2}\right]\Bigg|_{s=0}, \tag{24}$$

and finally, by substituting (23) in (24), yields

$$\begin{aligned} f(\sigma) = {} & \frac{1}{p\left(0, k_p, \alpha_1, \ldots, \alpha_{n-2}, \sigma\right)}\left[\frac{\partial p\left(s, k_p, \alpha_1, \ldots, \alpha_{n-2}, \sigma\right)}{\partial s} - \frac{p\left(0, k_p, \alpha_1, \ldots, \alpha_{n-2}, \sigma\right)}{q(0,\sigma)}\frac{\partial q(s,\sigma)}{\partial s}\right]^2\Bigg|_{s=0} \\ & + \frac{2}{q(0,\sigma)}\frac{\partial q(s,\sigma)}{\partial s}\left[\frac{\partial p\left(s, k_p, \alpha_1, \ldots, \alpha_{n-2}, \sigma\right)}{\partial s} - \frac{p\left(0, k_p, \alpha_1, \ldots, \alpha_{n-2}, \sigma\right)}{q(0,\sigma)}\frac{\partial q(s,\sigma)}{\partial s}\right]\Bigg|_{s=0} \\ & + \left[\frac{p\left(0, k_p, \alpha_1, \ldots, \alpha_{n-2}, \sigma\right)}{q(0,\sigma)}\frac{\partial^2 q(s,\sigma)}{\partial s^2}\right]\Bigg|_{s=0} - \left[\frac{\partial^2 p\left(s, k_p, \alpha_1, \ldots, \alpha_{n-2}, \sigma\right)}{\partial s^2}\right]\Bigg|_{s=0} = 0, \end{aligned} \tag{25}$$

that completes the proof. □

5. PR Controller Design for a Flexible Joint Arm

In this section, the conditions proposed to achieve the maximum decay rate σ^* are considered for the design of a Proportional Retarded control law implemented on a flexible joint robotic arm experimental platform.

5.1. Robot Dynamic Model. The schematic representation of the flexible joint robotic arm is given in Figure 2.

The notation used is as follows (for the sake of simplicity of notation, in the following, we will omit the time dependence of the functions). θ_1 and θ_2 are the angular positions of the rotating base and of the arm, respectively. J_1 is the moment of inertia of the rotating base and J_2 is the moment of inertia of the rotating arm. m denotes the mass of the arm, while l represents the arm length. g is the gravity constant, k_s is the spring stiffness, and M is the torque applied to the system. The motor torque M_m and the torque applied to the system M satisfy the relation $M = NM_m$, where N denotes the mechanical advantage of the pulley system.

Following the Euler–Lagrange formulation, the equations of motion of the flexible joint robotic arm can be derived as

$$M = J_1\ddot{\theta}_1 + J_2\left(\ddot{\theta}_1 + \ddot{\theta}_2\right) + \frac{mgl}{2}\sin\left(\theta_1 + \theta_2\right), \tag{26}$$

$$0 = J_2\left(\ddot{\theta}_1 + \ddot{\theta}_2\right) + k_s\theta_2 + \frac{mgl}{2}\sin\left(\theta_1 + \theta_2\right). \tag{27}$$

Besides, the control input voltage applied to the motor V and the torque M_m are related as follows:

$$M_m = \frac{k_m}{R_m}V - \frac{k_m^2 N}{R_m}\dot{\theta}_1, \tag{28}$$

where R_m symbolizes the armature resistance and k_m the torque constant of the motor. Based on the above relations, (26) and (27) are now of the form

$$\begin{aligned} \frac{Nk_m}{R_m}V &= \left(J_1 + J_2\right)\ddot{\theta}_1 + J_2\ddot{\theta}_2 + \frac{k_m^2 N^2}{R_m}\dot{\theta}_1 + \frac{mgl}{2}\sin\left(\theta_1 + \theta_2\right), \\ 0 &= J_2\left(\ddot{\theta}_1 + \ddot{\theta}_2\right) + k_s\theta_2 + \frac{mgl}{2}\sin\left(\theta_1 + \theta_2\right), \end{aligned} \tag{29}$$

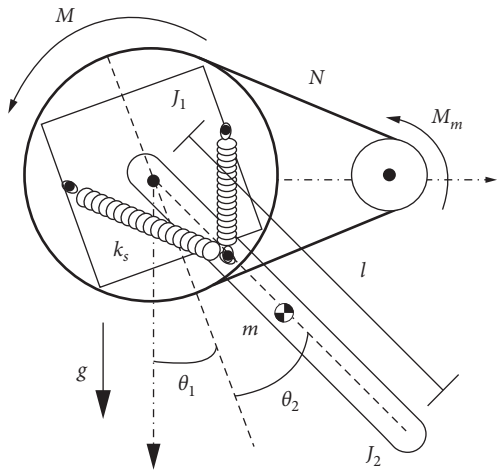

Figure 2: Schematic of a flexible joint robot arm.

or equivalently

$$\ddot{\theta}_1 = \kappa_2\theta_2 - \kappa_1\dot{\theta}_1 + \delta V, \tag{30}$$

$$\ddot{\theta}_2 = -\kappa_3\theta_2 - \kappa_4 \sin(\theta_1 + \theta_2) + \kappa_1\dot{\theta}_1 - \delta V, \tag{31}$$

where

$$\begin{aligned} \kappa_1 &= \frac{k_m^2 N^2}{J_1 R_m}, \\ \kappa_2 &= \frac{k_s}{J_1}, \\ \kappa_3 &= \frac{k_s(J_1 + J_2)}{J_1 J_2}, \\ \kappa_4 &= \frac{mgl}{2J_2}, \\ \delta &= \frac{k_m N}{J_1 R_m}. \end{aligned} \tag{32}$$

5.2. PR Controller Design. By performing the change of variables $x \coloneqq [x_1 x_2 x_3 x_4]^\top = [\theta_1 \dot{\theta}_1 \theta_2 \dot{\theta}_2]^\top$, systems (30) and (31) can be rewritten as

$$\dot{x} = f(x) + g(x)V, \tag{33}$$

where

$$f(x) = \begin{bmatrix} x_2 \\ -\kappa_1 x_2 + \kappa_2 x_3 \\ x_4 \\ \kappa_1 x_2 - \kappa_3 x_3 - \kappa_4 \sin(x_1 + x_3) \end{bmatrix},$$

$$g(x) = \begin{bmatrix} 0 \\ \delta \\ 0 \\ -\delta \end{bmatrix}. \tag{34}$$

The first stage in the design of the delayed controller is to transform nonlinear system (33) into a linear system via feedback linearization approach. Let us define

$$h(x) = x_1 + x_3, \tag{35}$$

as the output function. Denoting $L_f h(x)$ and $L_g h(x)$ as the Lie derivatives of function $h(x)$ with respect of the vector fields f and g, respectively (see [35]). Thus, differentiating the output function $h(x)$,

$$\dot{h}(x) = \frac{\partial h(x)}{\partial x}\dot{x} = L_f h(x) + L_g h(x) = x_2 + x_4, \tag{36}$$

and computing the higher order derivative of $h(x)$,

$$\begin{aligned} \ddot{h}(x) &= L_f^2 h(x), \\ h^{(3)}(x) &= L_f^3 h(x), \\ h^{(4)}(x) &= L_f^4 h(x) + V L_g L_f^3 h(x), \end{aligned} \tag{37}$$

where

$$\begin{aligned} L_f^2 h(x) &= (\kappa_2 - \kappa_3)x_3 - \kappa_4 \sin(x_1 + x_3), \\ L_f^3 h(x) &= -\kappa_4 (x_2 + x_4)\cos(x_1 + x_3) + (\kappa_2 - \kappa_3)x_4, \\ L_f^4 h(x) &= (\kappa_2 - \kappa_3)(\kappa_1 x_2 - \kappa_3 x_3) + \kappa_4 \sin(x_1 + x_3) \\ &\quad \cdot \left[(x_2 + x_4)^2 - (\kappa_2 - \kappa_3) + \kappa_4 \cos(x_1 + x_3)\right] \\ &\quad + \kappa_4 (\kappa_3 - \kappa_2) x_3 \cos(x_1 + x_3), \\ L_g L_f^3 h(x) &= -(\kappa_2 - \kappa_3)\delta. \end{aligned} \tag{38}$$

Hence, the system has relative degree four. Now, let us define the state transformation $z_1 = h(x)$, $z_2 = \dot{h}(x)$, $z_3 = h^{(2)}(x)$, and $z_4 = h^{(3)}(x)$, then it follows that

$$\begin{aligned} \dot{z}_1 &= L_f h(x), \\ \dot{z}_2 &= L_f^2 h(x), \\ \dot{z}_3 &= L_f^3 h(x), \\ \dot{z}_4 &= L_f^4 h(x) + V L_g L_f^3 h(x). \end{aligned} \tag{39}$$

Thus, the linearizing control function is of the form

$$V = \frac{1}{L_g L_f^3 h(x)}\left[u - L_f^4 h(x)\right]. \tag{40}$$

By denoting $h^*(x) = z_1^*$ as the desired trajectory and $h^{(j)*}(x) = z_{(j+1)}^*$, $j = 1, 2, 3, 4$, as its time derivatives, the errors functions are defined as $e_{z_j} = z_j - z_j^*$, then it follows

$$\begin{aligned} \dot{e}_{z_1} &= e_{z_2}, \\ \dot{e}_{z_2} &= e_{z_3}, \\ \dot{e}_{z_3} &= e_{z_4}, \\ \dot{e}_{z_4} &= u. \end{aligned} \tag{41}$$

Now, by proposing the delayed controller,

$$u_{\mathrm{PR}} = -k_p e_{z_1} + k_r e_{z_{1,\tau}} - \alpha_1 e_{z_3} - \alpha_2 e_{z_4}, \tag{42}$$

where the error $e_{z_{1,\tau}}$ is defined as

$$e_{z_1,\tau} = h(x_\tau) - h^*(x_\tau) = [x_1(t-\tau) + x_3(t-\tau)] - [x_1^*(t-\tau) + x_3^*(t-\tau)]. \tag{43}$$

Thus, system (41) in closed-loop, with control law (42), can be expressed as

$$\dot{e}_z = A_0 e_z + A_1 e_{z,\tau}, \tag{44}$$

where $e_z = [e_{z_1} e_{z_2} e_{z_3} e_{z_4}]^\top$ and

$$A_0 = \begin{bmatrix} 0 & 1 & 0 & 0 \\ 0 & 0 & 1 & 0 \\ 0 & 0 & 0 & 1 \\ -k_p & 0 & -\alpha_1 & -\alpha_2 \end{bmatrix}, \quad A_1 = \begin{bmatrix} 0 & 0 & 0 & 0 \\ 0 & 0 & 0 & 0 \\ 0 & 0 & 0 & 0 \\ k_r & 0 & 0 & 0 \end{bmatrix}. \tag{45}$$

The characteristic quasi-polynomial of system (44) is

$$Q(s, k_p, k_r, \alpha_1, \alpha_2) = p(s, k_p, \alpha_1, \alpha_2) + k_r q(s) e^{-s\tau}, \tag{46}$$

where $p(s, k_p, \alpha_1, \alpha_2) = s^4 + \alpha_2 s^3 + \alpha_1 s^2 + k_p$ and $q(s) = -1$. Now, using the change of variable $s = s - \sigma$, (46) takes the form

$$Q_\sigma(s, k_p, k_r, \alpha_1, \alpha_2) = p(s, k_p, \alpha_1, \alpha_2, \sigma) + k_r e^{\sigma\tau} q(s, \sigma) e^{-s\tau}, \tag{47}$$

where

$$\begin{aligned} p(s, k_p, \alpha_1, \alpha_2, \sigma) &= s^4 + (-4\sigma + \alpha_2)s^3 + (6\sigma^2 - 3\alpha_2\sigma + \alpha_1)s^2 \\ &\quad + (-4\sigma^3 + 3\alpha_2\sigma^2 - 2\alpha_1\sigma)s \\ &\quad + (\sigma^4 - \alpha_2\sigma^3 + \alpha_1\sigma^2 + k_p), \\ q(s, \sigma) &= -1. \end{aligned} \tag{48}$$

By Proposition 1, we have that when $s = 0$,

$$k_r = \frac{\sigma^4 - \alpha_2\sigma^3 + \alpha_1\sigma^2 + k_p}{e^{\sigma\tau}}, \tag{49}$$

while for $s = i\omega$

$$\tau = \frac{1}{\omega}\cot^{-1}\left(-\frac{\mathrm{Re}\{(p(i\omega, k_p, \alpha_1, \alpha_2, \sigma))/(q(i\omega, \sigma))\}}{\mathrm{Im}\{(p(i\omega, k_p, \alpha_1, \alpha_2, \sigma))/(q(i\omega, \sigma))\}}\right) + \frac{j\pi}{\omega},$$

$$k_r = \frac{1}{e^{\sigma\tau}\sin(\omega\tau)}\mathrm{Im}\left\{\frac{p(i\omega, k_p, \alpha_1, \alpha_2, \sigma)}{q(i\omega, \sigma)}\right\}, \tag{50}$$

where $j = 0, \pm 1, \pm 2, \ldots$ and

$$\begin{aligned} \mathrm{Re}\left\{\frac{p(i\omega, k_p, \alpha_1, \alpha_2, \sigma)}{q(i\omega, \sigma)}\right\} &= -\sigma^4 + \alpha_2\sigma^3 - (\alpha_1 - 6\omega^2)\sigma^2 \\ &\quad - 3\alpha_2\omega^2\sigma - \omega^4 + \alpha_1\omega^2 - k_p, \\ \mathrm{Im}\left\{\frac{p(i\omega, k_p, \alpha_1, \alpha_2, \sigma)}{q(i\omega, \sigma)}\right\} &= \omega[4\sigma^3 - 3\alpha_2\sigma^2 + (-4\omega^2 + 2\alpha_1)\sigma \\ &\quad + \alpha_2\omega^2]. \end{aligned} \tag{51}$$

According to Proposition 2 we first compute $Q_\sigma(s, k_p, k_r, \alpha_1, \alpha_2)|_{s=0}$, as well as its first and second partial derivatives, that is,

$$Q_\sigma(\cdot)\big|_{s=0} = e^{\sigma\tau}k_r = \sigma^4 - \alpha_2\sigma^3 + \alpha_1\sigma^2 + k_p, \tag{52}$$

$$\frac{\partial}{\partial s}Q_\sigma(\cdot)\bigg|_{s=0} = \tau e^{\sigma\tau}k_r = 4\sigma^3 - 3\alpha_2\sigma^2 + 2\alpha_1\sigma, \tag{53}$$

$$\frac{\partial^2}{\partial s^2}Q_\sigma(\cdot)\bigg|_{s=0} = \tau^2 e^{\sigma\tau}k_r = 12\sigma^2 - 6\alpha_2\sigma + 2\alpha_1. \tag{54}$$

From (52) and (53), we get

$$\tau = \frac{4\sigma^3 - 3\sigma^2\alpha_2 + 2\sigma\alpha_1}{\sigma^4 - \sigma^3\alpha_2 + \sigma^2\alpha_1 + k_p}, \tag{55}$$

and from (52) and (54), it follows that

$$\tau^2 = \frac{12\sigma^2 - 6\sigma\alpha_2 + 2\alpha_1}{\sigma^4 - \sigma^3\alpha_2 + \sigma^2\alpha_1 + k_p}. \tag{56}$$

Substituting (55) into (56), we have

$$\begin{aligned} f(\sigma) &= 4\sigma^6 - 6\sigma^5\alpha_2 + (2\alpha_1 + 3\alpha_2^2)\sigma^4 \\ &\quad - 4\alpha_2\alpha_1\sigma^3 + (2\alpha_1^2 - 12k_p)\sigma^2 + 6\alpha_2 k_p\sigma - 2\alpha_1 k_p. \end{aligned} \tag{57}$$

Summarizing, for given k_p, α_1, and α_2, then if σ^* is the minimum real solution of polynomial (57), then the gains of the controller that determine the σ^* stability of the system with a root of multiplicity at least three are established as

$$\tau^* = \frac{4(\sigma^*)^3 - 3(\sigma^*)^2\alpha_2 + 2\sigma^*\alpha_1}{(\sigma^*)^4 - (\sigma^*)^3\alpha_2 + (\sigma^*)^2\alpha_1 + k_p}, \tag{58}$$

$$k_r^* = \frac{\sigma^*(4(\sigma^*)^2 - 3\sigma^*\alpha_2 + 2\alpha_1)}{\tau^* e^{\sigma^*\tau^*}}. \tag{59}$$

In the previous procedure, analytic expressions to determine the optimal values of parameters k_r^*, τ^*, and σ^* were determined, but there are no words about parameters α_1, α_2, and k_p; thus, in the subsequent paragraphs, a simple methodology for preselection or approximation of these parameters is presented.

First, by computing the Maclaurin series $e^{-s\tau} = 1 - s\tau + ((\tau^2 s^2)/2) - ((\tau^3 s^3)/6)$ and substituting it in (47), we obtain the expression

$$Q_\sigma(s) = s^4 + \left(\alpha_2 + \frac{\tau^3 k_r}{6}\right)s^3 + \left(\alpha_1 - \frac{\tau^2 k_r}{2}\right)s^2 + (\tau k_r)s + \left(k_p - k_r\right). \tag{60}$$

Now, it is desirable to select the controller gains k_p, α_1, and α_2 in such a way that the dynamics of the close-loop system follow those of a proposed Hurwitz polynomial of the form

$$p_a(s) = \left(s^2 + 2\xi\omega_n s + \omega_n^2\right)^2 = s^4 + 4\xi\omega_n s^3 + \left(2\omega_n^2 + 4\xi^2\omega_n^2\right)s^2 + 4\xi\omega_n^3 s + \omega_n^4, \tag{61}$$

where $\xi, \omega_n > 0$. In order to match the dynamics of polynomials (60) and (61), the following parametrized conditions must be fulfilled:

$$k_p > \sqrt{\frac{\left(4\xi\omega_n^3\right)^3}{24\xi\omega_n} + \omega_n^4}, \tag{62}$$

$$\alpha_1 = 2\omega_n^2 + 4\xi^2\omega_n^2 + \frac{\left(4\xi\omega_n^3\right)^2}{2\left(k_p - \omega_n^4\right)}, \tag{63}$$

$$\alpha_2 = 4\xi\omega_n - \frac{\left(4\xi\omega_n^3\right)^3}{6\left(k_p - \omega_n\right)^2}. \tag{64}$$

Remark 1. It is worth mentioning, that expressions (62)–(64) can be considered only as a starting point to set the controller gains k_p, α_1, and α_2 and must be adapted according to the control designer expertise. On the other hand, expressions (57)–(59) guarantee to reach the maximal decay rate for given parameters k_p, α_1, and α_2.

6. Practical Implementation

In this section, the designed PR control law (40) is implemented in a flexible joint arm experimental platform using Matlab-Simulink, through a data acquisition device. The effectiveness of the proposed control law is assessed by means of tracking a rest-to-rest angular position reference trajectory. For comparative purposes, a feedback state control is designed and implemented in the experimental platform.

6.1. Experimental Setup. A block diagram of the experimental prototype is presented in Figure 3. The experimental platform incorporate a DC motor NISCA model NC5475, attached to a rotating base trough a belt pulley system with a 16 : 1 ratio. The flexible joint consists of a main arm attached to the rotating base by springs. The angular positions, of the rotating base and the arm, are measured by incremental encoders. The data acquisition task was performed by a

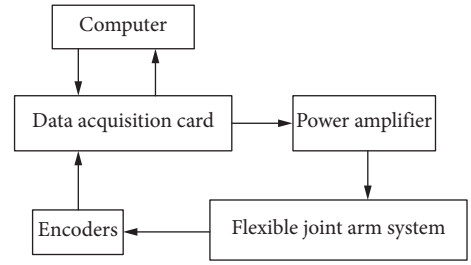

Figure 3: Diagram of the experimental platform architecture.

Sensoray 626 card. The control law was implemented in a Matlab-Simulink real time model, where the sampling period was fixed to be 0.001 s. The values of the flexible joint robotic arm parameters are $l = 0.5\,\text{m}$, $m = 0.1633\,\text{kg}$, $J_1 = 0.0136\,\text{kg}\cdot\text{m}^2$, $J_2 = 0.002405\,\text{kg}\cdot\text{m}^2$, $k_s = 4\,\text{N}\cdot\text{m/rad}$, and $N = 16$, while the motor parameters are $k_m = 0.0724\,\text{N}\cdot\text{m/A}$ and $R_m = 2.983\,\Omega$.

6.2. Feedback State Control. In order to compare PR control law (42) with a classical controller, we propose a feedback state control (FS):

$$u_{\text{FS}} = -\beta_1 e_{z_1} - \beta_2 e_{z_2} - \beta_3 e_{z_3} - \beta_4 e_{z_4}, \tag{65}$$

where the set of gains $[\beta_1, \beta_2, \beta_3, \beta_4]$ are positive constants. Using (40) and (41), we obtain the close-loop dynamic error:

$$e_{z_1}^{(4)} + \beta_4 e_{z_1}^{(3)} + \beta_3 \ddot{e}_{z_1} + \beta_2 \dot{e}_{z_1} + \beta_1 e_{z_1} = 0. \tag{66}$$

The characteristic polynomial is matched with a Hurwitz polynomial of the form

$$p_{\text{FL}}(s) = s^4 + \beta_4 s^3 + \beta_3 s^2 + \beta_2 s + \beta_1 = \left(s^2 + 2\zeta\varpi s + \varpi^2\right)^2. \tag{67}$$

The set of controller gains is chosen as follows:

$$\begin{aligned} \beta_1 &= \varpi^4, \\ \beta_2 &= 4\zeta\varpi^3, \\ \beta_3 &= 4\zeta^2\varpi^2 + 2\varpi^2, \\ \beta_4 &= 4\zeta\varpi. \end{aligned} \tag{68}$$

6.3. Experimental Results. The PR controller gains were selected as follows. We first proposed $\xi = 1.8$ and $\omega_n = 49$, and the gains k_p, α_1, and α_2 were selected from equations (62)–(64); after a slight adjustment, the gains were setted as $k_p = 4.5 \times 10^7$, $\alpha_1 = 5.7 \times 10^4$, and $\alpha_2 = 80$. On the other hand, the minimum real solution of (57) was $\sigma^* = 28.5495$, then using equations (58) and (59) we obtained the values $\tau^* = 0.0349$ and $k_r^* = 3.3 \times 10^7$.

In Figure 4, the σ-stability boundaries are depicted. The red mark represents the maximal achievable decay rate and corresponds to the place where all the σ-stable regions collapsed in a single point. According to (68), the FS controller gains were selected as follows $\zeta = 1.8$ and $\varpi = 52$.

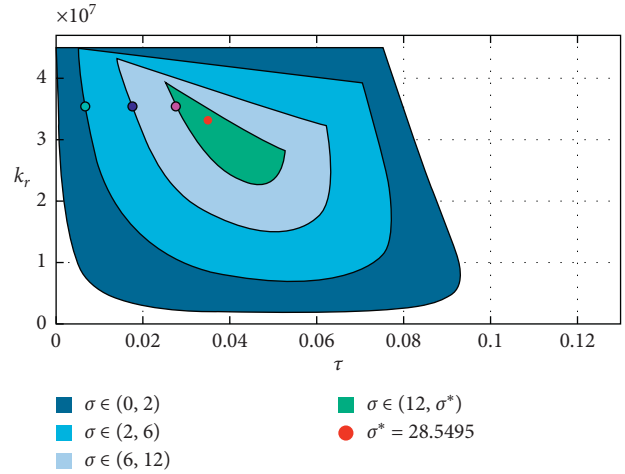

Figure 4: σ^*-stability region.

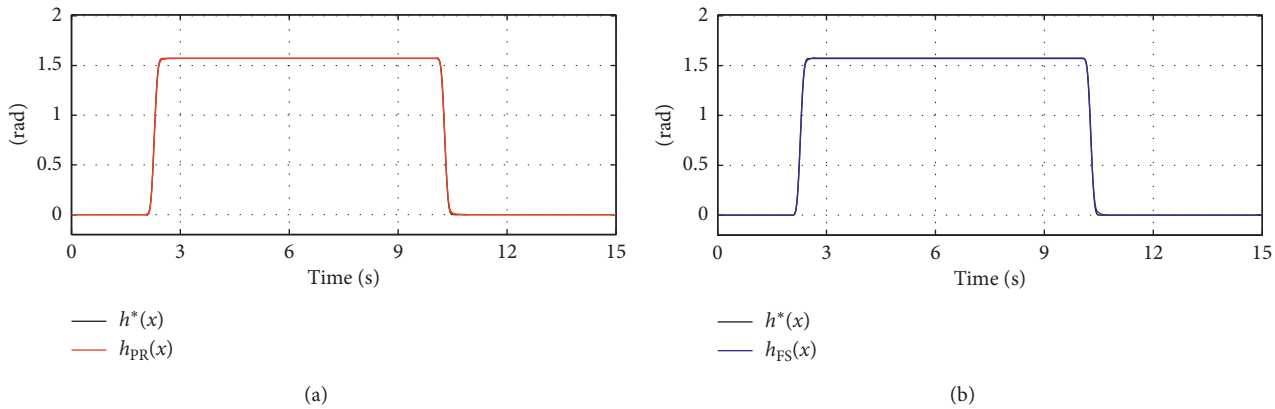

Figure 5: Trajectory tracking performance.

The initial conditions for both experiment PR and FL controllers are setting $\theta_1 = x_1(0) = 0$ and $\theta_2 = x_3(0) = 0$; this implies that output function (35) is $h(x) = 0$. The desired trajectory $h^*(x)$ starts at time $t = 0$ in the position $h^*(x) = 0$, when the time is $t = 1$, and it moves in 0.6 seconds. So, when $t = 1.6$ and $h^*(x) = \pi/2$, it remains in this position for 8 seconds and after this time the reference is moved to the initial location in 0.6 seconds, that is, $h^*(x) = 0$ when $t = 10.6$, and it remains in this position until the test is finished.

Vibrations are a common phenomenon in this class of systems, mainly when rest-to-rest point task is required. Figure 5(a) shows the PR controller performance, the output trajectory tracking $h_{PR}(x)$ depicted in red, and the desired trajectory $h^*(x)$ in black. In the same way, in Figure 5(b), the FL controller output $h_{FS}(x)$ is depicted in blue. We can notice that both outputs $h_{PR}(x)$ and $h_{FS}(x)$ smoothly follows the desired trajectory avoiding overshoot, as well as undesirable oscillations. The tracking trajectory errors e_{PR} (up) and e_{FS} (bottom) are shown in Figure 6. PR error, denoted by e_{PR}, is bounded in a neighborhood of $[-0.02, 0.02]$ rad, while FL error (e_{FS}) is bounded in a neighborhood of $[-0.02, 0.03]$ rad, and it shows some oscillations and a mayor amplitude in comparison with the PR controller.

PR voltage input (V_{PR}) is depicted in Figure 7(a) and the maximum amplitude of the signal is approximately $[-15, 15]$ Volts, and it does not present noise when the system is in the steady state, and FS voltage V_{FS} is shown in Figure 7(b). Here, we can notice similar performance of both V_{PR} and V_{FS} in amplitude and form, but V_{FS} shows a clear increase in noise and frequency: In order to clarify this statement, a Power Density Spectrum (PSD) of each voltage control is depicted in Figure 8. As we can observe, PR_{PSD} exhibits low-frequency components with a small peak at 7.7 Hz. On the other hand, FS_{PSD} shows more high-frequency components. Low-frequency components on the PR controller give us some advantages such as less wear on the actuators, less power consumption, and vibrations, among others. The above can be verified by observing Figures 9 and 10, where the performance of the system is evaluated by means of a quadratic index for both the error and the applied voltage.

Now, it is desirable to evaluate the performance of the flexible joint robotic platform in other points of the parametric space (τ, k_r). Here, we consider points with similar

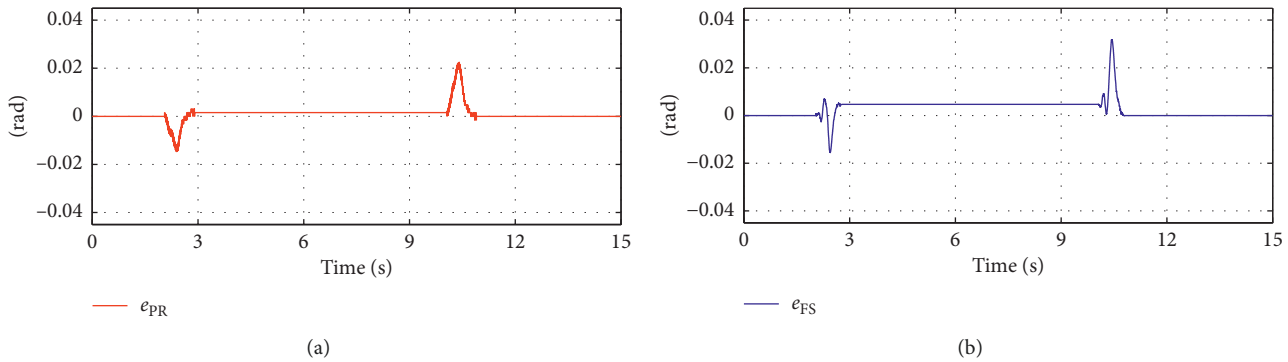

Figure 6: Tracking error.

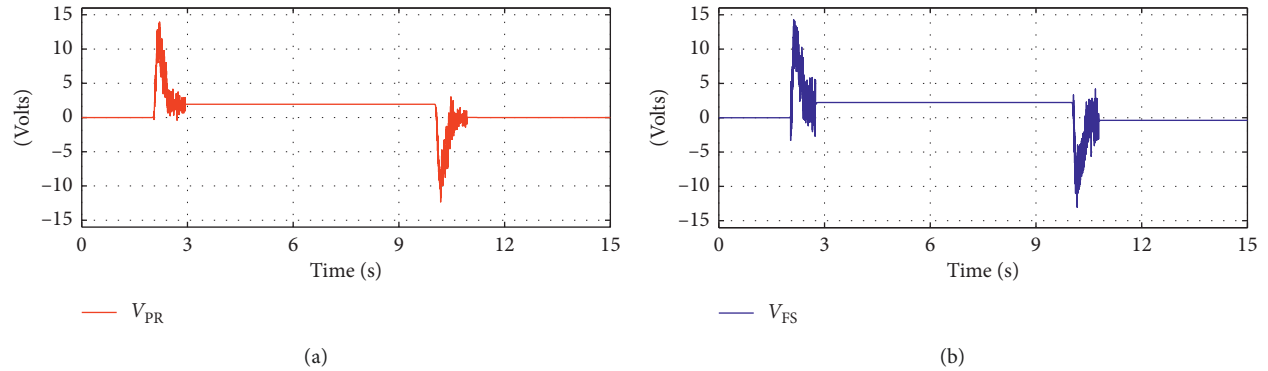

Figure 7: Control input voltage.

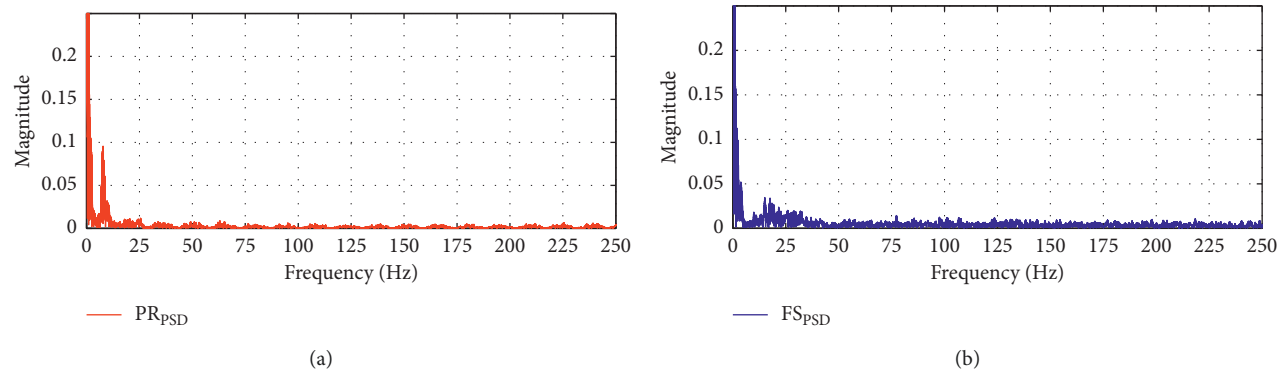

Figure 8: Power spectrum density.

control parameters but with different exponential decay rate σ and consequently a different delay τ. These points are depicted in Figure 4 and its control parameters are given in Table 1.

The system responses, at the selected points, are depicted in Figure 11, where it can be seen that the control tasks were carried out satisfactorily. Since each of the points corresponds to different σ-stable regions with a specific decay rate, the zoom at the bottom of Figure 11 allows us to note that the transient response of the system vanishes according to Table 1, and as expected, the system achieves the maximal decay rate at the point $\sigma^* = 28.5495$. A similar statement can be made, when the error signals are analyzed (see Figure 12).

Remark 2. The σ-stability approach provides us some benefits from the robustness perspective. Since the parameters τ^* and k_r^* are selected deep inside the stability region, the effect of parameter variations only affect the decay rate but not the stability property. This statement can

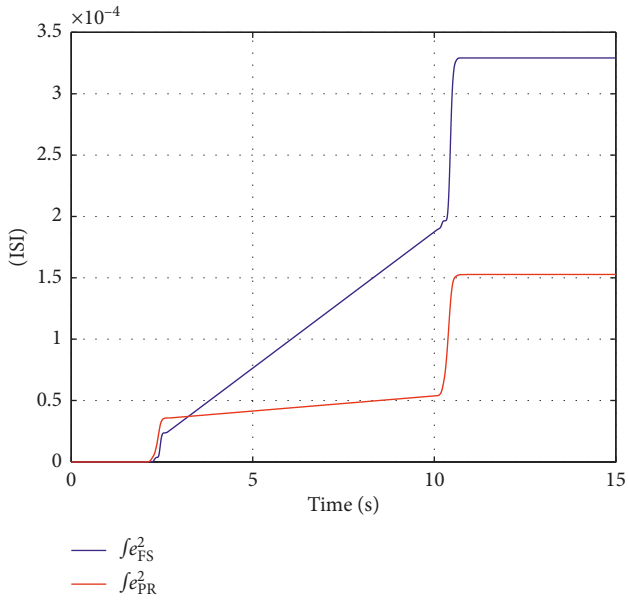

Figure 9: Performance index of the error.

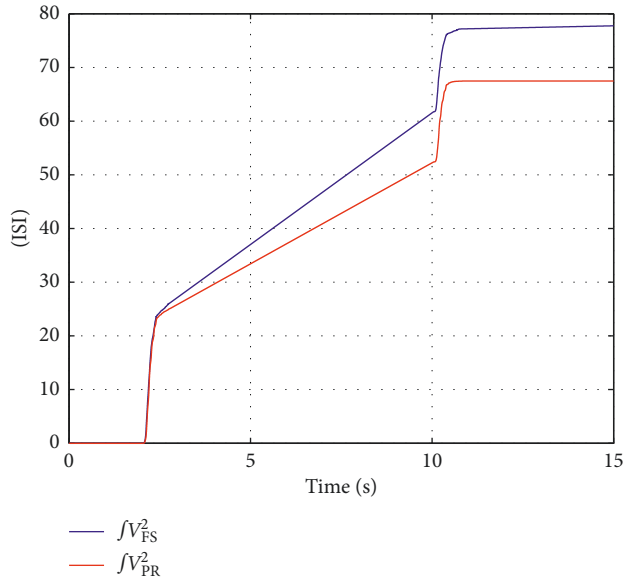

Figure 10: Performance index of the controller.

Table 1: Parameters (k_r, τ) and settling time.

	Parameters			Settling time
Color	σ	k_r	τ (s)	Time (s)
Cyan	2	3.5e7	0.006767	1.128
Blue	6	3.5e7	0.01775	0.947
Magenta	12	3.5e7	0.02784	0.655
Red	28.5495	3.3e7	0.0349	0.321

be verified in Figures 11 and 12, where the performance of the system is evaluated for parameters (τ, k_r) taken far from the point (τ^*, k_r^*). It can be appreciated that the further the control parameters are selected from the point (τ^*, k_r^*), the

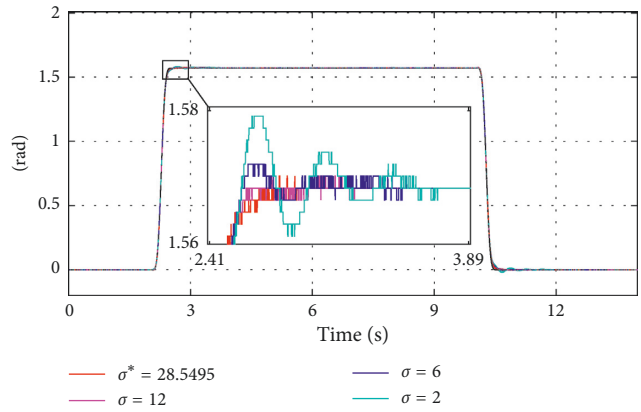

Figure 11: Trajectory tracking results.

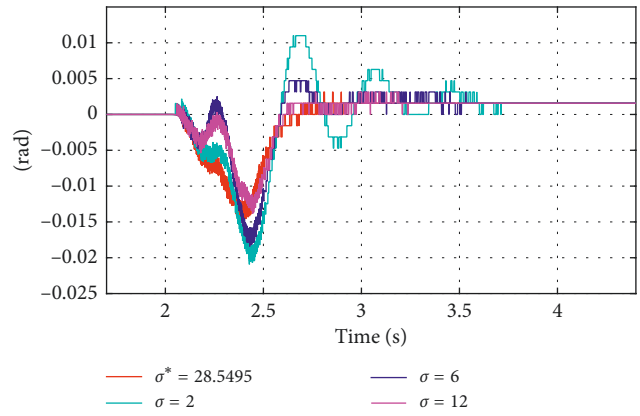

Figure 12: Tracking error signals.

greater the decay rate will be, but the stability of the system remains.

7. Conclusions

Analytic conditions for the design of proportional retarded controllers that guarantee reaching the optimal decay rate for a general class of LTI systems are presented. A detailed design of a proportional retarded controller, which shows the ease with which the proposed conditions can be computed and implemented, is developed for the control of an experimental platform that consists of a flexible joint robotic arm. The experimental results illustrate the effectiveness of the conditions and show remarkable tracking of rest-to-rest trajectories avoiding oscillations, noise, and overshoot.

Data Availability

All the data generated or analyzed during this study are included in this paper.

Conflicts of Interest

The authors declare that there are no conflicts of interest regarding the publication of this paper.

References

[1] R. Sipahi, S.-I. Niculescu, C. T. Abdallah, W. Michiels, and K. Gu, "Stability and stabilization of systems with time delay," *IEEE Control Systems*, vol. 31, no. 1, pp. 38–65, 2011.

[2] C. Abdallah, P. Dorato, J. Benites-Read, and R. Byrne, "Delayed positive feedback can stabilize oscillatory systems," in *Proceedings of the 1993 American Control Conference*, pp. 3106-3107, San Francisco, CA, USA, June 1993.

[3] V. Kharitonov, S.-I. Niculescu, J. Moreno, and W. Michiels, "Static output feedback stabilization: necessary conditions for multiple delay controllers," *IEEE Transactions on Automatic Control*, vol. 50, no. 1, pp. 82–86, 2005.

[4] S.-I. Niculescu and W. Michiels, "Some remarks on stabilizing a chain of integrators using multiple delays," in *Proceedings of the 2003 American Control Conference*, vol. 3, pp. 2664–2669, IEEE, Denver, CO, USA, June 2003.

[5] S.-I. Niculescu and W. Michiels, "Stabilizing a chain of integrators using multiple delays," *IEEE Transactions on Automatic Control*, vol. 49, no. 5, pp. 802–807, 2004.

[6] N. Olgac and M. E. Cavdaroglu, "Full-state feedback controller design with "delay scheduling" for cart-and-pendulum dynamics," *Mechatronics*, vol. 21, no. 1, pp. 38–47, 2011.

[7] K. Pyragas, "Continuous control of chaos by self-controlling feedback," *Physics Letters A*, vol. 170, no. 6, pp. 421–428, 1992.

[8] A. Galip Ulsoy, "Time-delayed control of SISO systems for improved stability margins," *Journal of Dynamic Systems, Measurement, and Control*, vol. 137, no. 4, Article ID 041014, 2015.

[9] K. Gu, V. Kharitonov, and J. Chen, "Stability of time-delay systems," *Addison-Wesley Series in Electrical and Computer Engineering: Control Engineering*, Springer-Verlag, New, York, NY, USA, 2003.

[10] V. L. Kharitonov, *Time Delay Systems: Lyapunov Functionals and Matrices*, Springer Science & Business Media, Berlin, Germany, 2013.

[11] K. J. Aström and T. Hägglund, *Advanced PID Control*, ISA–The Instrumentation, Systems and Automation Society, Research Triangle, CA, USA, 2006.

[12] C. Knospe, "PID control," *IEEE Control Systems Magazine*, vol. 26, no. 1, pp. 30-31, 2006.

[13] M. A. Johnson and M. H. Moradi, *PID Control*, Springer-Verlag, London, UK, 2005.

[14] H. Kokame and T. Mori, "Stability preserving transition from derivative feedback to its difference counterparts," *IFAC Proceedings Volumes*, vol. 35, no. 1, pp. 129–134, 2002.

[15] I. Suh and Z. Bien, "Proportional minus delay controller," *IEEE Transactions on Automatic Control*, vol. 24, no. 2, pp. 370–372, 1979.

[16] H. Suh and Z. Bien, "Use of time-delay actions in the controller design," *IEEE Transactions on Automatic Control*, vol. 25, no. 3, pp. 600–603, 1980.

[17] D. A. Irofti, K. Gu, I. Boussaada, and S.-I. Niculescu, "Some insights into the migration of double imaginary roots under small deviation of two parameters," *Automatica*, vol. 88, pp. 91–97, 2018.

[18] R. Villafuerte and S. Mondié, "Tuning the leading roots of a second order DC servomotor with proportional retarded control," *IFAC Proceedings Volumes*, vol. 43, no. 2, pp. 337–342, 2010.

[19] A. Ramirez, S. Mondie, and R. Garrido, "Proportional integral retarded control of second order linear systems," in *Proceedings of the 52nd IEEE Conference on Decision and Control*, pp. 2239–2244, IEEE, Florence, Italy, December 2013.

[20] J.-E. Hernández-Díez, C.-F. Méndez-Barrios, S. Mondié, S.-I. Niculescu, and E. J. González-Galván, "Proportional-delayed controllers design for LTI-systems: a geometric approach," *International Journal of Control*, vol. 91, no. 4, pp. 907–925, 2017.

[21] C.-I. Morarescu and S.-I. Niculescu, "Stability crossing curves of siso systems controlled by delayed output feedback," *Dynamic of Continous Discrete and Impulsive Systems Series B*, vol. 14, no. 5, p. 659, 2007.

[22] R. Villafuerte, S. Mondie, and R. Garrido, "Tuning of proportional retarded controllers: theory and experiments," *IEEE Transactions on Control Systems Technology*, vol. 21, no. 3, pp. 983–990, 2013.

[23] S. Mondié, R. Villafuerte, and R. Garrido, "Tuning and noise attenuation of a second order system using proportional retarded control," *IFAC Proceedings Volumes*, vol. 44, no. 1, pp. 10337–10342, 2011.

[24] A. Ramírez, R. Garrido, and S. Mondié, "Velocity control of servo systems using an integral retarded algorithm," *ISA Transactions*, vol. 58, pp. 357–366, 2015.

[25] A. Ramírez, R. Sipahi, S. Mondié, and R. Garrido, "Design of maximum decay rate for SISO systems with delayed output feedback using elimination theory," *IFAC-PapersOnLine*, vol. 48, no. 12, pp. 221–226, 2015.

[26] A. Ramirez, S. Mondie, R. Garrido, and R. Sipahi, "Design of proportional-integral-retarded (PIR) controllers for second-order LTI systems," *IEEE Transactions on Automatic Control*, vol. 61, no. 6, pp. 1688–1693, 2016.

[27] E. N. Gryazina, "The D-decomposition theory," *Automation and Remote Control*, vol. 65, no. 12, pp. 1872–1884, 2004.

[28] E. N. Gryazina and B. T. Polyak, "Stability regions in the parameter space: D-decomposition revisited," *Automatica*, vol. 42, no. 1, pp. 13–26, 2006.

[29] E. N. Gryazina, B. T. Polyak, and A. A. Tremba, "D-decomposition technique state-of-the-art," *Automation and Remote Control*, vol. 69, no. 12, pp. 1991–2026, 2008.

[30] J. Neimark, "D-decomposition of the space of quasipolynomials," *Applied Mathematics and Mechanics*, vol. 13, pp. 349–380, 1949.

[31] A. Ramírez, R. Garrido, and S. Mondié, "Integral retarded velocity control of DC servomotors," *IFAC Proceedings Volumes*, vol. 46, no. 3, pp. 558–563, 2013.

[32] R. Villafuerte, F. Medina, L. Vite, and B. Aguirre, "Tuning of a time-delayed controller for a general class of second-order LTI systems with dead-time," *IET Control Theory & Applications*, vol. 13, no. 3, pp. 451–457, 2019.

[33] M. Benosman and G. Le Vey, "Control of flexible manipulators: a survey," *Robotica*, vol. 22, no. 5, pp. 533–545, 2004.

[34] S. Ozgoli and H. Taghirad, "A survey on the control of flexible joint robots," *Asian Journal of Control*, vol. 8, no. 4, pp. 332–344, 2006.

[35] Isidori, *Nonlinear Control Systems*, Springer Science & Business Media, Berlin, Germany, 2013.

[36] H. Sira-Ramirez and S. K. Agrawal, *Differentially Flat Systems*, CRC Press, Boca Raton, FL, USA, 2004.